The Charge-Transfer States in a Stacked Nucleobase Dimer Complex: A Benchmark Study

ADÉLIA J. A. AQUINO,[1,2] DANA NACHTIGALLOVA,[3] PAVEL HOBZA,[3] DONALD G. TRUHLAR,[4] CHRISTOF HÄTTIG,[5] HANS LISCHKA[1,3]

[1]*Institute for Theoretical Chemistry, University of Vienna, Währinger Straße 17, A-1090 Vienna, Austria*

[2]*Institute of Soil Research, University of Natural Resources and Life Sciences Vienna, Peter-Jordan-Straße 82, A-1190 Vienna, Austria*

[3]*Institute of Organic Chemistry and Biochemistry, Academy of Sciences of the Czech Republic and Center for Biomolecules and Complex Molecular Systems, Flemingovo nam. 2, 166 10 Prague 6, Czech Republic*

[4]*Department of Chemistry and Supercomputing Institute, University of Minnesota, Minneapolis, Minnesota 55455-0431*

[5]*Lehrstuhl für Theoretische Chemie, Ruhr-Universität Bochum, Universitätsstrasse 150, D-44801 Bochum, Germany*

Received 9 August 2010; Revised 27 September 2010; Accepted 1 October 2010
DOI 10.1002/jcc.21702
Published online 29 November 2010 in Wiley Online Library (wileyonlinelibrary.com).

Abstract: Electronic singlet excitations of stacked adenine–thymine (AT) and guanine–cytosine (GC) complexes have been investigated with respect to local excitation and charge-transfer (CT) characters. Potential energy curves for rigid displacement of the nucleobases have been computed to establish the distance dependence of the CT states. The second-order algebraic diagrammatic construction [ADC(2)] method served as reference approach for comparison to a selected set of density functionals used within the time-dependent density functional theory (TD-DFT). Particular attention was dedicated to the performance of the recently developed family of M06 functionals. The calculations for the stacked complexes show that at the ADC(2) level, the lowest CT state is S_6 for the AT and as S_4 for the GC pair. At the reference geometry, the actual charge transferred is found to be 0.73 *e* for AT. In case of GC, this amount is much smaller (0.17 *e*). With increasing separation of the two nucleobases, the CT state is strongly destabilized. The M06-2X version provides a relatively good reproduction of the ADC(2) results. It avoids the serious overstabilization and overcrowding of the spectrum found with the B3LYP functional. On the other hand, M06-HF destabilizes the CT state too strongly. TD-DFT/M06-2X calculations in solution (heptane, isoquinoline, and water) using the polarizable continuum model show a stabilization of the CT state and an increase in CT character with increasing polarity of the solvent.

© 2010 Wiley Periodicals, Inc. J Comput Chem 32: 1217–1227, 2011

Key words: charge transfer; excited states; coupled cluster; DFT; stacked nucleobases

Additional Supporting Information may be found in the online version of this article.

Correspondence to: A. J. A. Aquino; e-mail: adelia.aquino@univie.ac.at or H. Lischka; e-mail: hans.lischka@univie.ac.at

Contract/grant sponsor: Austrian Science Fund [Special Research Programs F16 (Advanced Light Sources) and F41 (ViCoM)] and contract/grant number: P18411-N19
Contract/grant sponsor: German Research Foundation (priority program SPP 1315); contract/grant number: GE 1676/1-1
Contract/grant sponsors: Ministry of Education of the Czech Republic (Center for Biomolecules and Complex Molecular Systems, LC512) and Praemium Academiae of the Academy of Sciences of the Czech Republic awarded to PH in 2007
Contract/grant sponsor: Institute of Organic Chemistry and Biochemistry of the Academy of Sciences of the Czech Republic; contract/grant number: research project Z40550506
Contract/grant sponsor: U. S. National Science Foundation; contract/grant number: CHE09-56776
Contract/grant sponsor: Vienna Scientific Cluster; contract/grant numbers: 70019 and 70151

© 2010 Wiley Periodicals, Inc.

Introduction

The last decade has witnessed remarkable advances in the field of photophysics and photochemistry of nucleic acids in both theory and experiment. The nature of the electronically excited states of these systems is of major importance because of the fact that the reactivity of DNA bases in the excited state can lead to serious damage of the nucleic acids and to alteration of the genetic code. It is now well established that isolated nucleobases are photostable because of ultrafast (few ps) deactivation from the lowest excited singlet states to the electronic ground state because of the existence of ultrafast nonradiative relaxation mechanisms.[1–6]

Interaction of nucleobases in their excited states via interstrand hydrogen bonding and intrastrand stacking result in additional mechanisms of self-protection of nucleic acid bases from UV damage by opening new decay channels.[7–10] Time-resolved spectra of both single- and double-stranded DNA oligomers and polymers clearly demonstrate the existence of different excited state dynamics of bases in stacking interactions when compared with isolated DNA bases.[11,12] The nature of these interactions and their dynamics is, however, still a matter of intense discussion. Intrastrand excimer formation connected with charge-transfer (CT) character have played a major role in the interpretation of experiments, but delocalized excitons have also been proposed to play a role as well.[10] It follows that a number of questions still need to be answered, in particular, on (i) the character of excited states during the UV absorption process, (ii) the degree of delocalization, (iii) the role of geometry relaxation on the nature of an excited state, (iv) the CT effect in the excited state dynamics, and (v) the role of dark states.

Theoretical methods have played an important role in clarifying the mechanisms of the photostability of single nucleobases. High-level multireference methods such as complete active space self-consistent field, CAS with perturbation theory to second order (CASPT2), and multireference configuration interaction have been used.[3–6,13,14] Fleig et al.[15] have investigated the excited states of the nucleobases with the approximate coupled cluster singles-and-doubles method CC2.[16] Other computational research on the character of the excited states in stacking interactions has been published recently as well.[17–21] To investigate similar questions of photostability beyond single bases requires methods that are still accurate enough to properly describe excited states and the interactions of excited state molecules but are capable of treating significantly larger systems. Unfortunately, the size of these systems prevents the extensive use (e.g., see refs. 21–23) of the highly correlated methods just mentioned. In most cases, less time-consuming methods have to be applied.

Density functional theory (DFT) methods would be a natural choice for studying larger systems. For example, Tonzani and Schatz[24] used molecular dynamics simulations combined with time-dependent density functional theory (TD-DFT) calculations for the $(dA)_{11}$ oligomer, and absorption and emission spectra were calculated using the polarized continuum model (PCM) and TD-DFT/PBE0 on stacked dimers and trimers of adenine.[25] It has been suggested that geometry relaxation results in the localization of the originally delocalized excited state on a single base. However, the TD-DFT method requires a careful selection of the functional for the correct treatment of the CT character of the excited states. Standard functionals are known to fail.[26–28] Various attempts have been made to solve this problem to obtain a satisfactory description of CT in nucleobase oligomers. Extensive investigation of CT artifacts of the TD-DFT/PBE0 method can be found in ref. 29 together with successful applications of long-range corrections to remove the overstabilization of CT states. In calculations of $(dA)_2.(dT)_2$ oligomers, in which both hydrogen bonding and stacking interactions were considered,[30] the reliability of the PBE0 functional for describing the UV absorption spectrum was compared with that obtained from M05-2X calculations.[31] The recently introduced M06 suite of density functionals[32,33] has been shown to provide very good results for noncovalent interactions in general and, moreover, has been developed also for calculations of electronic excitations. The (TD-)DFT/M06 approach thus represents a promising tool for calculations of ground and excited state properties of different types of noncovalent complexes including various structural types of DNA base pairs and oligomers. Further, the method can be efficiently combined with polarizable continuum methods for a global description of the surrounding environment.

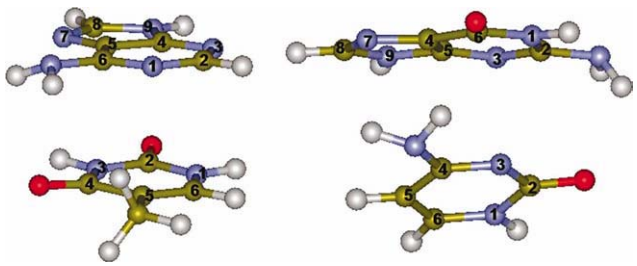
In spite of this progress, extensive testing and benchmarking of these and future DFT methods is necessary. The purpose of this work is to provide extended benchmark results for excitation energies, oscillator strengths, and characters of the low-lying singlet excited states of the nucleobase pairs, including the just-discussed CT states in excimer complexes of DNA bases. The difficulties of using multireference methods in such cases, which are caused by a prohibitive computational effort, have already been mentioned above. The approximate coupled cluster singles-and-doubles model CC2[16] and the second-order algebraic diagrammatic construction [ADC(2)][34] with the resolution of the identity have been proven as reliable and cost-effective methods for calculating excited states of larger molecules.[35,36]

As benchmark systems for exploring CT states, two stacked dimers, adenine–thymine (AT) and guanine–cytosine (GC), have been selected. Besides the characterization of vertical electronic excitations, the dependence of excited states on the distance between the stacked nucleobases, with particular emphasis on the CT states, is also investigated. These calculations should allow first assessments of the performance of computational methods concerning interactions over larger distances in DNA and concerning states delocalized over several base units.

This article is organized as follows: (i) a survey of the performance of various methods for vertical excitations in individual bases is given, (ii) based on this experience, vertical excitations in the stacked complexes are discussed, (iii) potential curves for rigid displacement between bases are presented, and (iv) solvent effects are investigated for selected cases.

Computational Details

The reference geometries of the AT and CG dimers (see Scheme 1 for structures and numbering) used in the vertical excitation calculations were taken from a ground state of B-DNA structure optimized at Møller-Plesset perturbation theory to second-order MP2/TZVPP level for AT[37] and from an experimental structure determined from NMR measurements for the CG dimer.[38] The nucleobases are not methylated.



Scheme 1. AT (left) and GC (right) complexes. [Color figure can be viewed in the online issue, which is available at wileyonlinelibrary.com.]

The calculations were performed at RI-CC2[16,39–41] (only for isolated base monomers), RI-ADC(2)[34,42–44], and TD-DFT[45–48] levels of theory. In the last case, the hybrid functionals B3-LYP[49] and PBE0[50] and the recently developed M06-2X[32] and M06-HF[33] functionals were selected. The RI-CC2 and RI-ADC(2) methods are computationally less expensive modifications of the coupled cluster theory with single and double excitations. The RI method,[39] applied for ADC(2) and CC2, is important as it decreases the computational effort for the time-consuming two-electron integrals considerably. The advantage of the ADC(2) method over CC2 in the present context of calculating a large number of excited states is the use of a Hermitian secular matrix which is constructed by many body perturbation theory. Thus, it was chosen as the major reference method for comparison with the TD-DFT results. The calculations have been performed using the SVP[51] and TZVP[52] basis sets. The SVP basis provides a cost-effective choice for performing calculations on larger systems whereas the TZVP basis enhances the flexibility of the valence orbitals. As the description of Rydberg states is out of the aim of the present work, no extra diffuse functions for their description were added to the basis. The geometry of the isolated bases adenine, thymine, guanine, and cytosine were fully optimized at the MP2/TZVP level. All calculations were performed in C_1 point-group symmetry and only singlet excitations were considered.

The assignment of the excitations (local or CT) was performed by considering the weight of the orbital excitation and the corresponding character of the orbitals. Cases of similar weights of different configurations to a given state are indicated in the tables. Potential curves were computed for vertical displacement of the stacked AT and GC structures along the $A(N_9)$–$T(O_9)$ distance in AT and the $G(C_5)$–$C(C_4)$ distance in GC (see Scheme 1). This distance is 3.154 Å in the reference geometry of AT and 3.104 Å in the GC reference structure. Intermonomer distances R were selected in the interval of 2.5–5.0 Å for both AT and GC complexes using a maximum of 12 points for each curve. The 10 lowest singlet excited states within the basis set used were calculated at each distance using the RI-ADC(2), M06-2X, M06-HF, PBE0, and B3-LYP methods and the SVP basis set. The final calculations were performed at the RI-ADC(2)/TZVP and M06-2X/TZVP levels. Atomic charges were calculated for both AT and GC through fits to the electrostatic potential calculated at spherical shells of grid points around the atoms using Bragg-Slater atomic radii.[53] These charges are denoted below as ESP charges.

Calculations based on the PCM[54,55] using the linear response method of Cammi et al.[56] were performed for the AT and GC complexes using the M06-2X functional and the TZVP basis set. Three different solvents, heptane (dielectric constant $\varepsilon = 1.920$), isoquinoline ($\varepsilon = 10.430$), and water ($\varepsilon = 78.39$) were selected using UA0 atomic radii (united atom topological model) of the universal force field[57] to carry out single-point calculations at the reference geometry of AT and GC for 10 excited singlet states. Nonequilibrium PCM calculations were performed at the TD-DFT level.[58] The present treatment treats solvation only in terms of bulk electrostatic effects and does not consider the geometry relaxation in solution. Corrections for hydrogen bonding, dispersion, and geometry relaxation in solution could be significant[59] but they are beyond the present scope. The TURBOMOLE program suite[60] has been used for the RI-CC2, RI-ADC(2), RI-MP2, TD-DFT/B3LYP, and TD-DFT/PBE0 calculations. The TD-DFT calculations for M06-2X and M06-HF functionals were carried out using a development version of Gaussian.[61]

Results and Discussion

Vertical Excitations of Isolated Bases

The vertical singlet excitation energies of the monomers were computed using the RI-CC2, RI-ADC(2), and TD-DFT methods. Tables 1 and 2, Supporting Information Tables 1S and 2S collect results and compare them with those obtained from CASPT2 calculations and with available experimental data. For a more extended discussion of the spectra of isolated nucleobases including a semiclassical simulation of the vibrational broadening see ref. 68 Cartesian geometries of optimized MP2/TZVP structures used in these calculations are given in the Supporting Information (Tables A–D).

Adenine

Only the N(9)H tautomer was considered as it corresponds to the tautomer treated in the stacked dimer, which appears in naturally occurred nucleic acids and has also been found as the major form both in gas phase and in solution.[69] The lowest vertical excited state (S_1) of adenine corresponds to an n-π^* excitation for all methods used. In the CASPT2 calculations of Fulscher et al.,[70] the S_1 state is of π-π^* character. However, a recent, more extended CASPT2 study on adenine[71] shows (Table 1) that the S_1 state is of n-π^* nature in agreement with RI-CC2 results of Fleig et al.[15] The S_2 and S_3 states are two energetically closely located π-π^* excitations where the latter [described as transition between the highest occupied molecular orbital (HOMO) and the lowest unoccupied orbital (LUMO)] has a significantly larger intensity.

Guanine

As for adenine, only the 9H tautomer was investigated. Different from adenine, for guanine, the π-π^* state is S_1 for all methods used in this work, excepted for M06-HF, which gives a too low n-π^* transition. The S_2 state is of n-π^* character for all methods, again with exception of M06-HF. The S_1 π-π^* excitation is of type HOMO $-$ LUMO $+$ 1. In contrast to adenine, both lowest

Table 1. Vertical Excitations Energies (eV) and Oscillator Strengths (In Parentheses) for the Three Lowest Singlet Excited States of Adenine and Guanine Using Different Methods and the TZVP Basis Set.

State	RI-ADC(2)	RI-CC2	M06-2X	M06-HF	CASPT2	Exp.
			Adenine			
S_1	5.09 (0.006)	5.17 (0.004)	5.27 (0.006)	5.56 (0.009)	4.96 (0.0037)[a]	
	n-π^*	n-π^*	n-π^*	n-π^*	n-π^*	
S_2	5.22 (0.035)	5.29 (0.003)	5.42 (0.294)	5.65 (0.313)	5.16 (0.0042)[a]	5.07[b]; 4.92[c]
	π-π^*	π-π^*	π-π^*	π-π^*	π-π^*	
S_3	5.33 (0.305)	5.42 (0.301)	5.57 (0.009)	5.86 (0.044)	5.35 (0.1747)[a]	
	π-π^*	π-π^*	π-π^*	π-π^*	π-π^*	
			Guanine			
S_1	5.05 (0.229)	5.19 (0.190)	5.23 (0.189)	4.89 (0.000)	4.93 (0.158)[d]	4.37[c]; 4.50[e]
	π-π^*	π-π^*	π-π^*	n-π^*	π-π^*	
S_2	5.27 (0.001)	5.55 (0.002)	5.36 (0.002)	5.43 (0.213)	5.54 (0.002)[d]	
	n-π^*	n-π^*	n-π^*	π-π^*	n-π^*	
S_3	5.63 (0.327)	5.71 (0.288)	5.70 (0.321)	6.03 (0.432)	5.77 (0.145)[d]	5.07[e]
	π-π^*	π-π^*	π-π^*	π-π^*	π-π^*	

[a]Ref. 71
[b]Ref. 63
[c]Ref. 64
[d]Ref. 62
[e]Ref. 65

π-π^* transitions have comparable intensities. Recent CASPT2 calculations on guanine[62] also give the order π-π^*, n-π^*, and π-π^* as the excitations for S_1, S_2, and S_3 states, respectively.

Thymine

For thymine, the S_1, S_2, and S_3 states correspond to n-π^*, π-π^*, and n-π^* excitations, respectively, for all methods used in this study (Table 2). Similar results have been obtained in the RI-CC2 study by Fleig et al.[15] The excitation energies shown in Table 2 demonstrate that the three excited states are well separated. A characteristic feature of thymine and also of cytosine discussed below is the occurrence of two low-lying n-π^* states. The n orbitals are mostly located on the oxygen atoms.

Cytosine

All computed vertical singlet excitation energies collected in Table 2 show the $\pi\pi^*$ state to be the lowest one. This state is followed closely by the second excited state (S_2), which corresponds to an nπ^* excitation. The third excited state (S_3) is again of n-π^* type. The n orbitals occurring in the two n-π^* excita-

Table 2. Vertical Excitations Energies (eV) and Oscillator Strengths (In Parentheses) for the Three Lowest Singlet Excited States of the Thymine and Cytosine Using Different Methods and the TZVP Basis Set.

State	RI-ADC(2)	RI-CC2	M06-2X	M06-HF	CASPT2	Exp.
			Thymine			
S_1	4.68 (0.000)	4.94 (0.000)	4.95 (0.000)	4.62 (0.000)	4.81[a]	4.70[b]
	n-π^*	n-π^*	n-π^*	n-π^*	π-π^*	
S_2	5.31 (0.254)	5.40 (0.197)	5.33 (0.204)	5.51 (0.267)	4.97[a]	
	π-π^*	π-π^*	π-π^*	π-π^*	n-π^*	
S_3	6.10 (0.000)	6.34 (0.000)	6.26 (0.000)	5.86 (0.000)	5.99[a]	
	n-π^*	n-π^*	n-π^*	n-π^*	π-π^*	
			Cytosine			
S_1	4.57 (0.057)	4.76 (0.055)	4.99 (0.074)	5.19 (0.100)	4.50[c] (0.065)	4.66[d]
	π-π^*	π-π^*	π-π^*	π-π^*	π-π^*	
S_2	4.76 (0.002)	4.96 (0.002)	5.17 (0.003)	5.28 (0.001)	4.88[c] (0.001)	
	n-π^*	n-π^*	n-π^*	n-π^*	n-π^*	
S_3	5.17 (0.003)	5.36 (0.002)	5.75 (0.000)	5.43 (0.000)	5.23[c] (0.003)	
	n-π^*	n-π^*	n-π^*	n-π^*	n-π^*	

[a]Ref. 4
[b]Ref. 67
[c]Ref. 66
[d]Ref. 65

Table 3. Vertical Excitations Energies (eV) and Oscillator Strengths *f* for the 10 Lowest Excited Singlet States of AT Obtained With Different Methods and the TZVP Basis Set.

	ADC(2)		M06-2X		M06-HF		PBE0	B3LYP
State	Δ*E*/assign[a]	*f*	Δ*E*/assign[a]	*f*	Δ*E*/assign[a]	*f*	Δ*E*/assign[a]	Δ*E*/assign[a]
S_1	4.72/Tn-Tπ^*	0.002	5.04/Tn-Tπ^*	0.001	4.72/Tn-Tπ^*	0.000	4.54/**A**π-**T**π^*	4.33/**A**π-**T**π^*
S_2	5.06/An-Aπ^*	0.018	5.20/Tπ-Tπ^*; **A**π-**T**π^*[b]	0.028	5.39/Tπ-Tπ^*	0.023	4.90/Tn-Tπ^*	4.79/Tn-Tπ^*
S_3	5.14/Aπ-Aπ^*	0.028	5.30/An-Aπ	0.007	5.59/An-Aπ^*	0.034	5.01/An-Aπ^*	4.88/Aπ–Aπ^*
S_4	5.21/Aπ-Aπ^*	0.024	5.38/**A**π-**T**π^*; Tπ-Tπ^*[b]	0.172	5.64/Aπ-Aπ^*	0.357	5.03/An-Aπ^*	4.89/An-Aπ^*
S_5	5.32/Tπ-Tπ^*	0.347	5.46/Aπ-Aπ^*	0.146	5.81/Aπ–Aπ^*	0.021	5.16/Aπ–Aπ^*	5.04/Aπ–Aπ^*
S_6	5.64/**A**π-**T**π^*	0.047	5.55/Aπ-Aπ^*	0.034	5.99/An-Aπ^*	0.002	5.26/**T**π-**A**π^*	5.08/**T**π-**A**π^*
S_7	5.77/An-Aπ^*	0.004	5.89/An-Aπ^*	0.003	6.03/Tn-Tπ^*	0.000	5.36/Aπ-Aπ^*	5.15/**An**-**T**π^*
S_8	6.10/An-Aπ^*	0.002	6.06/**T**π-**A**π^*	0.014	6.41/An-Aπ^*	0.005	5.42/**An**-**T**π^*	5.24/Aπ–Aπ^*
S_9	6.13/Tn-Tπ^*	0.001	6.30/An-Aπ^*	0.006	6.58/**A**π-**T**π^*	0.074	5.70/An-Aπ^*	5.52/**A**π-**T**π^*
S_{10}	6.22/**T**π-**A**π^*	0.005	6.36/Tn-Tπ^*	0.001	6.65/Aπ-Aπ^*	0.062	5.77/**A**π-**T**π^*	5.58/An-Aπ^*

CT states are highlighted in bold.
[a]Letters A and T of adenine and thymine, respectively, are used to identify the orbital localization.
[b]The two excitations contributions have similar weight.

tions are mostly distributed on N(3) and O. In the CASPT2 results,[72,73] the S_1, S_2, and S_3 excited states correspond to π-π^*, π-π^*, and n-π^* excitations, respectively.

Vertical Excitations in the Adenine–Thymine Complex

Vertical excitations energies, oscillator strengths, and state assignments are collected in Table 3 for the 10 lowest vertical singlet excitations of the AT complex for the different methods and the TZVP basis used. In Supporting Information Table 3S, RI-ADC(2) results are presented for the SVP basis. A comparison of the TZVP results with those obtained with the smaller SVP basis is of interest in view of future investigations on larger stacked oligomers. As already mentioned, the RI-CC2 calculations were not performed for the stacked structures as the RI-ADC(2) method gives very similar results and is computationally more efficient. Therefore, the RI-ADC(2) method was taken as reference for the analysis of the TD-DFT methods.

Comparison of the excitation energies of the AT complex (Table 3) to those of the isolated monomers discussed before (Tables 1 and 2) illustrates the shifts of the local excitations. These shifts are caused by environmental changes induced by the interacting bases and by geometry changes because of the use of optimized geometries of the isolated bases and experimental/optimized geometries in the stacked system. Most of the transitions can be characterized as either n-π^* or π-π^* type being mainly localized on one of the bases. However, as expected, a few transitions are of mixed nature and display CT character.

A correlation diagram between excitations in the isolated nucleobases and those observed in the AT complex is displayed in Figure 1 for the RI-ADC(2) approach. Inspection of this figure shows that the S_1, S_2, and S_3 excited states in thymine correspond to the S_1, S_5, and S_9 excited states in the AT complex. Similarly, states S_1, S_2, and S_3 of adenine are related to the states S_2, S_3, and S_4 states in AT. The energy shifts from the isolated base to the complex are relatively small amounting to about 0.1 eV or less. The excitation energies in thymine are lower than the corresponding energies in the dimer, while the corresponding excitation energies in adenine are larger. The transition energies obtained through the RI-ADC(2)/SVP approach (Supporting Information Table 3S) are always slightly higher (about 0.1–0.2 eV) than the corresponding TZVP values

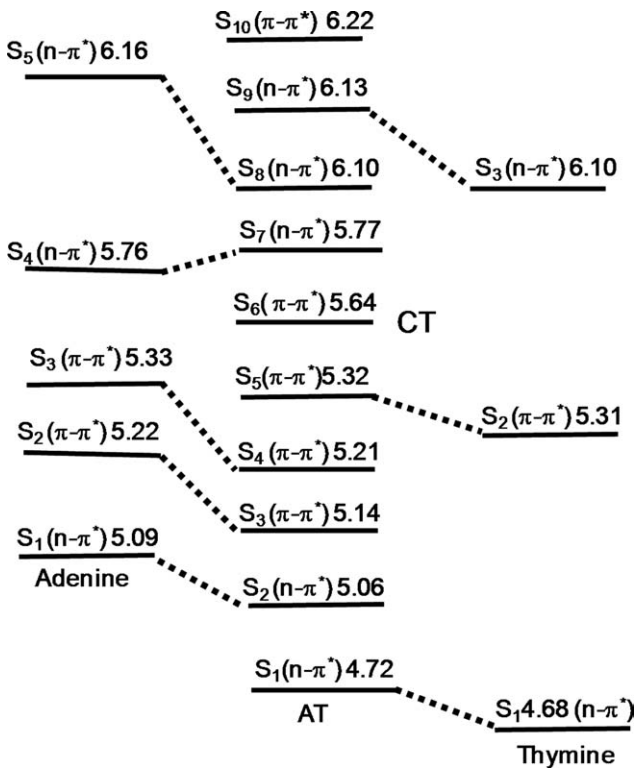


Figure 1. RI-ADC(2)/TZVP correlation diagram for excited states between isolated monomers and the AT complex in gas phase.

Table 4. ADC(2)/TZVP Charge Transfer (*e*) in the AT and GC Pairs, Respectively, Based on ESP Charges and Computed at the Reference Geometry.

	Charge	
State	A → T	G → C
S_1	0.018	0.009
S_2	0.068	0.073
S_3	0.076	0.071
S_4	0.063	0.170
S_5	0.056	0.063
S_6	0.730	0.126
S_7	0.081	0.055
S_8	0.043	0.279
S_9	0.019	−0.041
S_{10}	−0.097	0.066

(Table 3). Note as well that the CT state is moved from S_6 in the TZVP calculation to S_7 in SVP. The lowest singlet excited state S_1 is dominated by a local excitation n-π^* in thymine for the RI-ADC(2), M06-2X, and M06-HF methods with the n orbital located mainly on the lone pairs of the oxygen atoms of the pyrimidine ring. A completely different behavior is found for PBE0 and B3LYP as the S_1 state is a CT excitation between the π orbitals localized on adenine and thymine (Aπ–Tπ^*). The S_2 state corresponds to a local n-π^* excitation in adenine for RI-ADC(2) but is the lowest π-π^* excitation for M06-HF. For M06-2X, the S_2 state contains a mixing of π-π^* excitations each being localized in one of the base moieties. Therefore, this excitation can be described as an excitonic coupling between two π-π^* excitations. For the RI-ADC(2) calculations, the remaining S_3, S_4, S_7, and S_8 states correspond to local n-π^* or π-π^* excitations in adenine and the S_5 and S_9 states refer to π-π^* and n-π^* excitations on thymine, respectively. Two nonlocal CT excitations were observed in the RI-ADC(2) calculations for the S_6 and S_{10} states. The S_6 state is characterized by an excitation from the π orbital localized on adenine into the π^* orbital of thymine. On the other hand, the S_{10} CT state is an excitation from a π orbital in thymine to a π^* orbital on adenine. It is important to point out, therefore, that in this latter case, adenine is not the charge donor as observed for the state S_6 just mentioned above.

Excitations that are not localized on a single monomer are observed for the S_2, S_4, and S_8 states in the calculations carried out by the M06-2X method; however, the M06-2X calculations also show contributions from localized excitations in the S_2 and S_4 states. A clean CT state is observed only in case of the state S_8. In this case, the CT occurs in the direction from thymine to adenine. In the M06-HF approach, only state S_9 corresponds to a nonlocal CT excitation with CT from adenine to thymine. All remaining excited states are local excitations. The PBE0 and B3LYP functionals lead to four nonlocal excitations, and the first excited state has already CT character. In both methods, the CT process occurs from thymine to adenine in the S_6 state.

The CT is characterized by means of ESP charges computed at the RI-ADC(2)/TZVP level (Table 4). The CT is clearly seen for S_6 amounting to 0.73 *e*. The density difference plot between S_6 and S_0 (Fig. 2a) illustrates this CT from A to T in the π-π^* states very well.

Vertical Excitations in the Guanine–Cytosine Complex

Vertical excitation energies, oscillator strengths, and state assignments are shown in Table 5 for the 10 lowest vertical singlet excitations of the GC complex for the various methods and the TZVP basis used. In Supporting Information Table 3S, RI-ADC(2) results are presented for the SVP basis. Comparing the RI-ADC(2) excitation energies of the GC complex with those to the isolated bases (Tables 1 and 2), it is observed (see Fig. 3) that the S_1, S_2, and S_3 excited states in cytosine correspond to the S_1, S_2, and S_6 excited states in the complex. Similarly, states S_1, S_2, and S_3 in guanine are related to the states S_3, S_5, and S_7 in GC. The excitation energies for the isolated monomer and in the complex are quite close in both cases. The excitation energies in cytosine are lower than the corresponding energies in the dimer, while the corresponding excitation energies in guanine are larger than in the dimer. Similar to the AT case, the transition energies obtained with the RI-ADC(2)/SVP approach (Supporting Information Table 3S) are always slightly higher (about 0.1–0.2 eV) than the corresponding TZVP values. It is observed that the CT state is moved from S_4 in the TZVP calculation to S_6 in SVP.

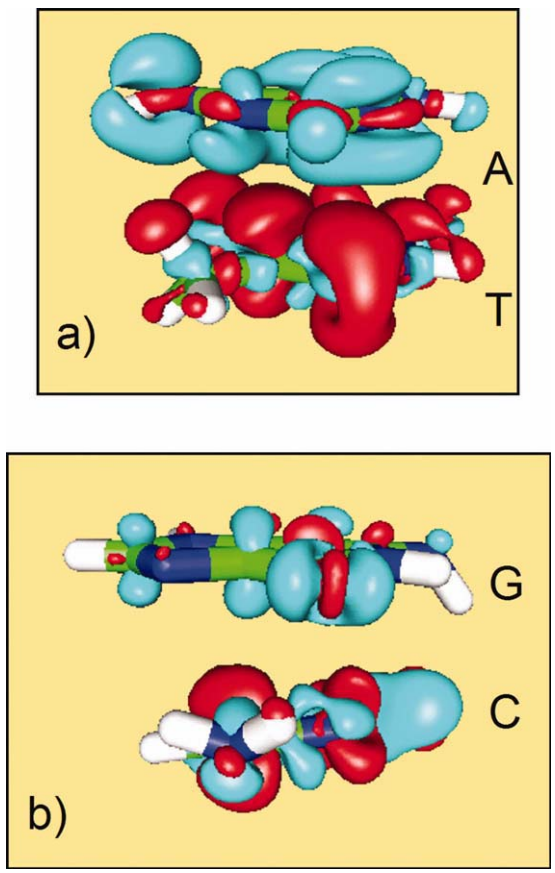


Figure 2. RI-ADC(2)/TZVP density difference plots between the densities of (a) AT, S_6, and S_0 and (b) GC, S_4, and S_0 in gas phase; Contour values: turquoise (light gray): −0.002 *e*, red (dark gray): 0.002 *e*. [Color figure can be viewed in the online issue, which is available at wileyonlinelibrary.com.]

Table 5. Vertical Excitations Energies (eV) and Oscillator Strengths *f* for 10 Lowest Excited Singlet States of GC Obtained With Different Methods and the TZVP Basis Set.

	ADC(2)		M06-2X		M06-HF		PBE0	B3LYP
State	Δ*E*/assign[a]	*F*	Δ*E*/assign[a]	*f*	Δ*E*/assign[a]	*f*	Δ*E*/assign[a]	Δ*E*/assign[a]
S_1	4.68/Cπ-Cπ*	0.034	4.99/**G**π-**C**π*	0.008	5.02/Gn-Gπ*	0.001	4.25/**G**π-**C**π*	4.04/**G**π-**C**π*
S_2	4.91/CnGπ-Cπ*	0.011	5.13/Cπ-Cπ*	0.039	5.29/Cπ-Cπ*	0.049	4.86/Cπ-Cπ*	4.73/Cπ-Cπ*
S_3	5.00/Gπ-Gπ*	0.050	5.27/Cn-Cπ*	0.024	5.39/Gπ-Gπ*	0.047	5.00/Cn-Cπ*	4.88/Cn-Cπ*
S_4	5.21/**G**π-**C**π*; Cn-Cπ*[b]	0.128	5.30/Gπ-Gπ*	0.086	5.45/Cn-Cπ*; Gπ-Gπ*[b]	0.065	5.07/Gπ-Gπ*	4.97/Gπ-Gπ*
S_5	5.24/Gn-Gπ*	0.010	5.40/Gn-Gπ*	0.001	5.73/Cn-Cπ*	0.002	5.22/Gπ-Gπ*	5.07/Gπ-Gπ*
S_6	5.25/Cn-Cπ*	0.039	5.56/Gπ-Gπ*	0.234	5.88/Gπ-Gπ*	0.300	5.36/Gn-Gπ*	5.20/**G**π-**C**π*; **Gn-C**π*[b]
S_7	5.46/Gπ-Gπ*	0.231	5.89/Cπ-Cπ*	0.102	6.07/Cπ-Cπ*; **G**π-**C**π*[b]	0.177	5.43/Cπ-Cπ*	5.24/Cn-Cπ*
S_8	5.52/Cπ-Cπ*	0.093	5.96/Cn-Cπ*	0.006	6.28/Gn-Gπ*	0.006	5.49/Cn-Cπ*	5.26/Gn-Gπ*; Cπ-Cπ*[b]
S_9	5.80/Cn-Cπ*	0.004	6.30/**G**π-**C**π*	0.038	6.42/**G**π-**C**π*; Cπ-Cπ*[b]	0.043	5.62/**G**π-**C**π*	5.38/**Gn-C**π*; **G**π-**C**π*[b]
S_{10}	5.99/Gn-Gπ*	0.002	6.36/Gπ-Gπ*	0.007	6.59/Cπ-Cπ*	0.311	5.66/**Gn-C**π*	5.40/**G**π-**C**π*

CT states are highlighted in bold.

[a]Letters C and G of cytosine and guanine, respectively, are used to identify in what monomer the orbital is localized.

[b]The two excitations contributions have similar weight.

The lowest singlet excited state corresponds at the RI-ADC(2) level to a π-π* transition in cytosine. For M06-HF, the S_1 state is related to a n-π* excitation in guanine, while for the M06-2X, PBE0, and B3LYP functional, the excitation in S_1 is described as a CT from an occupied π orbital in guanine to a virtual π* orbital in cytosine. For RI-ADC(2), the excitation into S_2 involves an excitation from an orbital with mixed G/C character to a π* orbital located on cytosine. The excited states S_3, S_5, and S_8 refer to local n-π* or π-π* excitations of guanine in the RI-ADC(2) calculation. S_4 is a CT excitation. Note, however, that there is also a local n-π* excitation on cytosine that contributes with similar weight to the overall excitation process in this state. Excited state CT appears in the M06-HF method for states S_7 and S_9. In both the cases, there is also a contribution by a local cytosine π-π* excitation. For the PBE0 and B3LYP approaches, CT excitations are observed in addition to the S_1 state already mentioned in states S_9 and S_{10} for PBE0 and S_6, S_9, and S_{10} for B3LYP. The CT is directed from guanine to cytosine in all methods used here.

The CT computed for GC by means of ESP charges (Table 4) is much less pronounced than in the AT case and amounts to only 0.17 *e* for S_4. However, this value increases substantially at larger distances R_{GC} reaching values of 0.8 *e*. Additionally, CT is noted for the states S_6 and S_8, which is not clearly recognizable in the analysis of the orbital excitations shown in Table 5. The density difference plot between S_4 and S_0 is shown in Figure 2b. In this case, the amount of charge transferred is significantly less than for AT and the mixed character of the electronic excitation is clearly seen.

Potential Energy Curves

Potential curves for the 10 lowest excited states of the AT and GC dimers were computed at the RI-ADC(2) M06-2X, M06-HF, PBE0, and B3LYP levels. Results for RI-ADC(2)/TZVP, M06-2X/TZVP, and PBE0/SVP are collected in Figures 4 and 5. Curves obtained with RI-ADC(2)/SVP (AT and GC, Supporting Information Figs. 1S and 4S), M06-HF/SVP (AT and GC, Supporting Information Figs. 2S and 5S), and B3LYP/SVP (AT, Supporting Information Fig. 3S) are available in the Supporting Information. CT states are indicated in the figures by red circles.

AT Complex

Potential curves for the AT complex are shown in Figure 4 and Supporting Information Figure 1S. The reference distance for

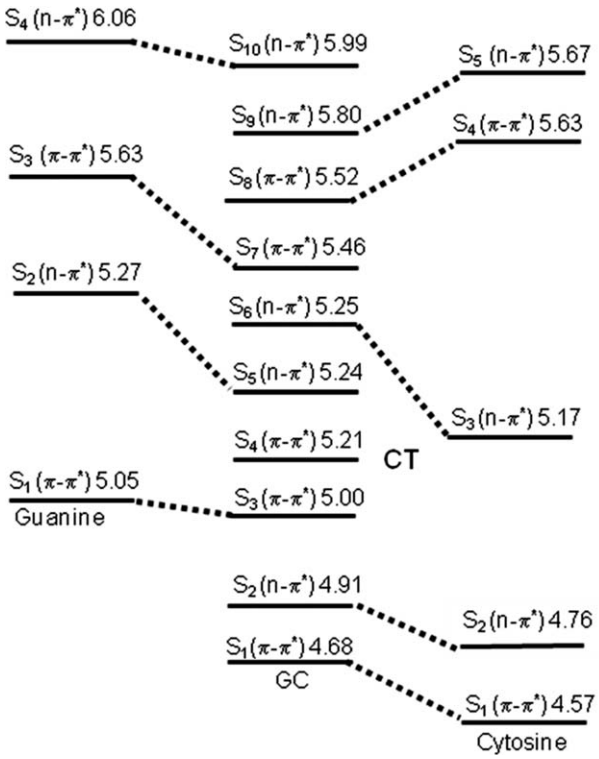


Figure 3. RI-ADC(2)/TZVP correlation diagram for excited states between isolated monomers and the GC complex in gas phase.

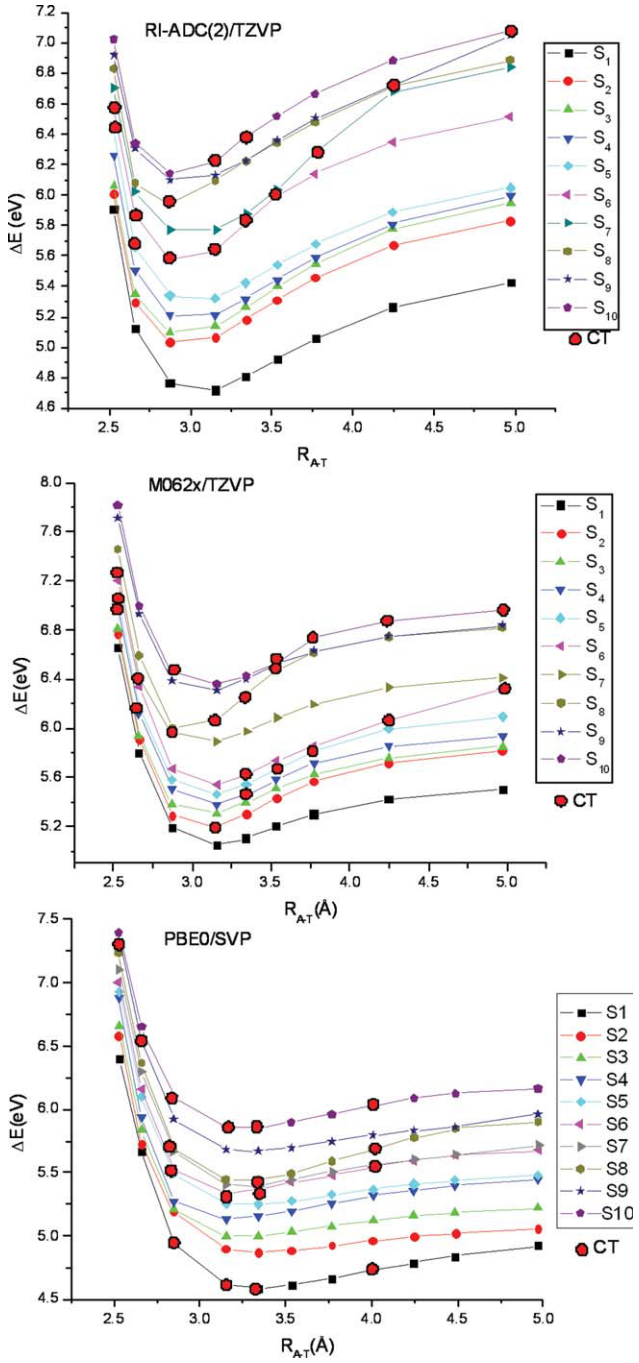


Figure 4. Potential energy curves for rigid separation in the intermolecular distance R_{AT} for the lowest 10 excited singlet states for AT in gas phase. The red circles indicate the CT state.

which the assignment of vertical excitations has been performed in the previous section is 3.154 Å. At this point, the CT state is located in S_6 of the RI-ADC(2) curve. With increasing distance R_{AT} of adenine and thymine, the CT state is strongly destabilized because of the increasing charge separation. At 3.65 Å, this state switches to S_7 and reaches S_{10} at a distance of 5 Å. At distances smaller than the reference distance, the CT character remains basically in S_6. A small part of the second CT curve characterized by the opposite CT direction can be seen at R = 3.154 Å and the following point (S_{10}). Because of the steeply increasing energy of the CT curves, this state moves out of the window of 10 excited states. Using the SVP basis with the RI-ADC(2) method (Supporting Information Fig. 1S) leads to similar shapes of all potential curves. The CT curve is also reproduced very well with this basis.

In the M06-2X curve, the Aπ–Tπ* CT state is distributed between the S_2 and S_4 states at 3.15 Å. The energetic overstabilization of this state when compared with the RI-ADC(2) result continues along the whole curve. The same happens for the second CT state (Tπ–Aπ*) which is S_8 at the reference geometry. For the M06-HF method, as expected from the analysis of vertical excitations, the whole CT curve is too strongly destabilized and only three points of the CT state can be seen in the 10-state window (Supporting Information Fig. 2S). The good results obtained with M06-2X are especially encouraging in light of its good performance for the noncovalent interactions in the ground state of biomolecules.[74–76] The PBE0 results displayed in Figure 4 show several CT states, the lowest one as S_1. An even stronger artificial overstabilization of CT states is found for B3LYP curves (Supporting Information Fig. 3S).

The remaining states had been characterized as local excitations for the vertical excitations (Table 3). In these cases, this local character is kept for the entire potential curves.

GC Complex

The analysis of the GC case follows the lines of discussion for the AT complex. Potential curves for GC are shown in Figure 5, Supporting Information Figures 4S and 5S. The reference distance for which the assignment of vertical excitations has been performed in the previous sections is 3.104 Å. In the reference RI-ADC(2) curve, the S_4 state is found to have CT character at the reference geometry when compared with S_6 for AT. Because of a stronger destabilization, it reaches S_{10} for R = 5 Å similar to the AT case. As for the AT complex, the SVP basis in combination with the RI-ADC(2) method (Supporting Information Fig. 4S) gives similar shapes for all potential curves, including the CT case.

In agreement with the observations made for the vertical excitations (Table 4), the entire CT curve computed with the M06-2X method (Fig. 5) is shifted to lower state numbers when compared with the RI-ADC(2) reference. A second CT state (also of Gπ–Cπ* character) is found at the M06-2X level as well, which follows exclusively S_9. As in the case of AT, the PBE0 results displayed in Figure 5 show the lowest CT state as S_1. The M06-HF CT curve (Supporting Information Fig. 5S) is energetically too high.

The remaining localized excitations can be analyzed on the basis of the assignment given for the vertical excitations collected in Table 4.

Solvation Effects on Charge Transfer Singlet States

To investigate the environmental effect on the CT process, the PCM method together with the TD-DFT/M06-2X/TZVP

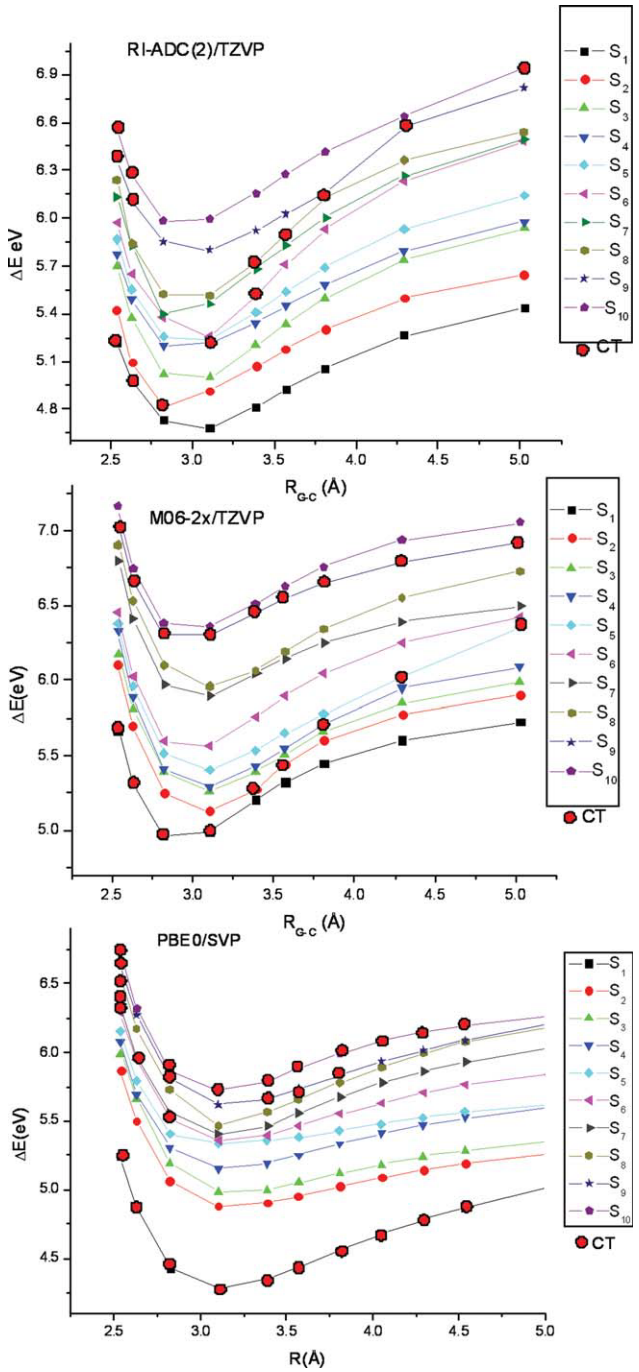


Figure 5. Potential energy curves for rigid separation in the intermolecular distance R_{CG} for the lowest 10 excited singlet states for GC in gas phase. The red circles indicate the CT state.

approach was used. The solvents *n*-heptane, isoquinoline, and water were chosen. Results for the vertical excitation in AT and GC, respectively, computed at the reference geometry are collected in Table 6. For comparison with excitation energies of the isolated complexes, see Tables 3 and 5. The vertical excitation energies for the isolated nucleobases in solution are collected in Supporting Information Table 4S. The energetic shifts with respect to the isolated complexes are relatively small (few hundredths of an eV up to 0.1–0.2 eV) for all excitations when compared with the isolated complex and blue shifts are observed in most cases. n-π^* states are more strongly blue shifted with increasing solvent polarity than π-π^* states. Such solvent shifts for the localized excitations are in good agreement with those computed for other aromatic systems (see ref. 77). In case of AT, the CT state, which is distributed over S_2 and S_4 for the isolated cluster, is stabilized relative to the other states in isoquinoline and water and appears as the lowest excited state in these solvents. For GC, the CT state is already S_1 in the isolated complex and it is 0.14 eV below the second lowest state; in isoquinoline and water, this is increased to 0.17–0.18 eV. The analysis of Table 6 also shows that the amount of CT character is increasing with the polarity of the solvent. The heptane solution gives a similar characterization of excited states in terms of orbital excitations as in the gas phase, whereas in isoquinoline and water, additional configurations with CT character are introduced into the π^* orbital into which the excitation takes place.

Conclusions

A systematic survey on the character of the electronic states in DNA bases and the stacked dimers adenine/thymine and guanine/cytosine has been performed. The vertical excitation energies of the excited singlet states of the AT and GC pairs have been calculated both at a reference geometry and as a function of the distance between the nucleobase pairs. In addition, at the reference geometry, we present oscillator strengths and an analysis of the dominant configurations in each of the states. The assignment of electronically excited states in terms of their localized or delocalized character is of great interest for the understanding of the defect dynamics in DNA. Benchmark data have been created using the RI-ADC(2) method, which is found to be a very good and efficient method for the calculation of excited states for molecular systems of the size of nucleobase dimers and beyond. The calculations for the stacked complexes show that the lowest CT state is located at this level of theory at S_6 for the AT and at S_4 for the GC pair. At the reference geometry, the actual charge transferred is found to be 0.73 *e* for AT. In case of GC, this amount is much smaller (0.17 *e*). With increasing separation of the two nucleobases, the CT state is strongly destabilized.

A selected set of density functionals was critically tested concerning their performance in the computation of CT states. In particular, the reliability of the newly developed family of M06 functionals was in the focus of these tests. The calculations showed that the M06-2X version provides a relatively good reproduction of the RI-ADC(2) results. It avoids the serious overstabilization and overcrowding of the spectrum found with the B3LYP method. PBE0 is already an improvement in comparison with B3LYP but is also not satisfactory overall. Especially, the observed destabilization of the CT states with increasing distance is much too weak for PBE0 when compared

Table 6. Liquid-Phase Excitation Energies and Oscillator Strengths for Electronic Transitions in AT and GC Computed With the M06-2X/TZVP/PCM Approach.

	Heptane		Isoquinoline		Water	
State	ΔE (eV)/assign	f	ΔE (eV)/assign	f	ΔE/assign (eV)	f
			AT			
S_1	5.12/Tn-Tπ^*	0.009	5.20/**A**π-**TA**π^*	0.025	5.16/**A**π-**TA**π^*	0.034
S_2	5.16/**A**π-**T**π^*; Tπ-Tπ^*	0.033	5.28/Tπ-TAπ^*	0.002	5.33/Tπ-TAπ^*	0.215
S_3	5.32/Tπ-Tπ^*	0.307	5.39/Tn-TAπ^*	0.232	5.34/Tn-TAπ^*	0.157
S_4	5.36/An-Aπ^*	0.062	5.45/An-ATπ^*; AnTπ^*	0.041	5.46/An-ATπ^*	0.014
S_5	5.47/Aπ-Aπ^*; **A**π-**T**π^*	0.087	5.53/Aπ-Aπ^*	0.016	5.53/Aπ-Aπ^*	0.017
S_6	5.53/Aπ-Aπ^*	0.027	5.58/Aπ-TAπ^*	0.066	5.60/Aπ-TAπ^*	0.062
S_7	5.94/An-Aπ^*	0.004	5.95/Tπ-TAπ^*	0.009	5.91/Tπ-TAπ^*	0.012
S_8	6.02/**Tπ-ATπ^***	0.019	6.02/An-Aπ^*	0.004	6.04/An-Aπ^*	0.005
S_9	6.36/An-Aπ^*	0.017	6.45/Tπ-Tπ^*	0.025	6.42/Tπ-Tπ^*	0.051
S_{10}	6.42/Tπ-Tπ^*	0.012	6.48/An-TAπ^*	0.014	6.51/AnTπ-ATπ^*	0.031
			GC			
S_1	5.02/**G**π-**C**π^*; CπCπ^*	0.019	5.07/**G**π-**C**π^*	0.015	5.05/**G**π-**C**π^*	0.019
S_2	5.16/Cπ-Cπ^*	0.084	5.25/Cπ-Cπ^*	0.107	5.22/Cπ-Cπ^*	0.184
S_3	5.30/Gπ-Gπ^*	0.112	5.38/**G**π-**C**π^*; GπGπ^*	0.039	5.39/**G**π-**C**π^*; Gπ-Gπ^*	0.026
S_4	5.36/Cn-Cπ^*	0.015	5.54/Cn-Cπ^*	0.022	5.53/Gπ-Gπ^*	0.293
S_5	5.50/Gπ-Gπ^*	0.320	5.58/Gπ-Gπ^*	0.215	5.61/Cn-Gπ-Cπ^*	0.017
S_6	5.50/Gn-Gπ^*	0.002	5.68/Gn-Gπ^*	0.002	5.73/Gn-Gπ^*	0.002
S_7	5.92/Cπ-Cπ^*	0.153	6.10/Cπ-Cπ^*	0.080	6.10/Cπ-Cπ^*	0.099
S_8	6.06/Cn-Cπ^*	0.005	6.21/Cn-R;Cn-Cπ^*	0.007	6.26/Cn-Cπ^*	0.038
S_9	6.31/**G**π-**C**π^*	0.107	6.34/**G**π-**C**π^*	0.144	6.30/**G**π-**C**π^*	0.229
S_{10}	6.40/Cπ-Cπ^*	0.148	6.44/**G**π-**C**π^*; **C**π-**G**π^*	0.063	6.42/**G**π-**C**π^*; **C**π-**G**π^*	0.039

CT states are highlighted in bold.

with RI-ADC(2) and M06-2X. The M06-HF method destabilizes the CT states too strongly so that it appears only marginally in the upper part of the 10-state energy window.

In summary, the results and analysis presented in this work should open research in the direction of (i) investigating the effect of geometry relaxation and concomitant energetic stabilization of the CT states and (ii) embedding relevant base oligomer clusters into an extended DNA environment using quantum mechanical/molecular mechanics[78–80] techniques.

References

1. Ullrich, S.; Schultz, T.; Zgierski, M. Z.; Stolow, A. J Am Chem Soc 2004, 126, 2262.
2. Canuel, C.; Mons, M.; Piuzzi, F.; Tardivel, B.; Dimicoli, I.; Elhanine, M. J Chem Phys 2005, 122, 074316.
3. Barbatti, M.; Lischka, H. J Am Chem Soc 2008, 130, 6831.
4. Perun, S.; Sobolewski, A. L.; Domcke, W. J Phys Chem A 2006, 110, 13238.
5. Hudock, H. R.; Levine, B. G.; Thompson, A. L.; Satzger, H.; Townsend, D.; Gador, N.; Ullrich, S.; Stolow, A.; Martinez, T. J. J Phys Chem A 2007, 111, 8500.
6. Merchán, M.; González-Luque, R.; Climent, T.; Serrano-Andrés, L.; Rodríguez, E.; Reguero, M.; Peláez, D. J Phys Chem B 2006, 110, 26471.
7. Crespo-Hernández, C. E.; Cohen, B.; Hare, P. M.; Kohler, B. Chem Rev 2004, 104, 1977.
8. Pecourt, J. M. L.; Peon, J.; Kohler, B. J Am Chem Soc 2001, 123, 5166.
9. Markovitsi, D.; Gustavsson, T.; Talbot, F. Photochem Photobiol Sci 2007, 6, 717.
10. Markovitsi, D.; Talbot, F.; Gustavsson, T.; Onidas, D.; Lazzarotto, E.; Marguet, S. Nature 2006, 441, E7.
11. Takaya, T.; Su, C.; de La Harpe, K.; Crespo-Hernandez, C. E.; Kohler, B. Proc Natl Acad Sci USA 2008, 105, 10285.
12. Markovitsi, D.; Onidas, D.; Gustavsson, T.; Talbot, F.; Lazzarotto, E. J Am Chem Soc 2005, 127, 17130.
13. Marian, C. M. J Chem Phys 2005, 122, 104314.
14. Szymczak, J. J.; Barbatti, M.; Hoo, J. T. S.; Adkins, J. A.; Windus, T. L.; Nachtigallova, D.; Lischka, H. J Phys Chem A 2009, 113, 12686.
15. Fleig, T.; Knecht, S.; Hättig, C. J Phys Chem A 2007, 111, 5482.
16. Christiansen, O.; Koch, H.; Jorgensen, P. Chem Phys Lett 1995, 243, 409.
17. Nachtigallova, D.; Hobza, P.; Ritze, H. H. PCCP 2008, 10, 5689.
18. Ritze, H. H.; Hobza, P.; Nachtigallova, D. PCCP 2007, 9, 1672.
19. Boggio-Pasqua, M.; Groenhof, G.; Schafer, L. V.; Grubmuller, H.; Robb, M. A. J Am Chem Soc 2007, 129, 10996.
20. Serrano-Perez, J. J.; Gonzalez-Ramirez, I.; Coto, P. B.; Merchan, M.; Serrano-Andres, L. J Phys Chem B 2008, 112, 14096.
21. Roca-Sanjuan, D.; Olaso-Gonzalez, G.; Gonzalez-Ramirez, I.; Serrano-Andres, L.; Merchan, M. J Am Chem Soc 2008, 130, 10768.
22. Olaso-Gonzalez, G.; Merchan, M.; Serrano-Andres, L. J Am Chem Soc 2009, 131, 4368.
23. Sobolewski, A. L.; Domcke, W. PCCP 2004, 6, 2763.
24. Tonzani, S.; Schatz, G. C. J Am Chem Soc 2008, 130, 7607.
25. Improta, R. Phys Chem Chem Phys 2008, 10, 2656.
26. Dreuw, A.; Head-Gordon, M. J Am Chem Soc 2004, 126, 4007.
27. Tozer, D. J. J Chem Phys 2003, 119, 12697.
28. Lange, A.; Herbert, J. M. JCTC 2007, 3, 1680.

29. Lange, A. W.; Herbert, J. M. J Am Chem Soc 2009, 131, 3913.
30. Santoro, F.; Barone, V.; Improta, R. Chemphyschem 2008, 9, 2531.
31. Zhao, Y.; Schultz, N. E.; Truhlar, D. G. JCTC 2006, 2, 364.
32. Zhao, Y.; Truhlar, D. G. Theor Chem Acc 2008, 120, 215.
33. Zhao, Y.; Truhlar, D. G. J Phys Chem A 2006, 110, 13126.
34. Trofimov, A. B.; Schirmer, J. J Phys B: At Mol Opt Phys 1995, 28, 2299.
35. Sobolewski, A. L.; Domcke, W.; Hättig, C. J Phys Chem A 2006, 110, 6301.
36. Aquino, A. J. A.; Lischka, H.; Hättig, C. J Phys Chem A 2005, 109, 3201.
37. Hobza, P.; Jurecka, P. J Am Chem Soc 2003, 125 15608.
38. Zidek, L.; Wu, H. H.; Feigon, J.; Sklenar, V. J Biomol NMR 2001, 21, 153.
39. Hättig, C. J Chem Phys 2003, 118, 7751.
40. Köhn, A.; Hättig, C. J Chem Phys 2003, 119, 5021.
41. Hättig, C.; Weigend, F. J Chem Phys 2000, 113, 5154.
42. Hattig, C. PCCP 2005, 7, 59.
43. Trofimov, A. B.; Schirmer, J. Chem Phys 1997, 214, 153.
44. Trofimov, A. B.; Schirmer, J. Chem Phys 1977, 224, 175.
45. Casida, M. E. Time-Dependent Density-Functional Response Theory for Molecules; World Scientific: Singapore, 1995.
46. Bauernschmitt, R.; Ahlrichs, R. Chem Phys Lett 1996, 256, 454.
47. Furche, F.; Ahlrichs, R. J Chem Phys 2002, 117, 7433.
48. Runge, E.; Gross, E. K. U. Phys Rev Lett 1984, 52, 997.
49. Becke, A. D. J Chem Phys 1993, 98, 5648.
50. Perdew, J. P.; Burke, K.; Ernzerhof, M. Phys Rev Lett 1996, 77, 3865.
51. Schafer, A.; Horn, H.; Ahlrichs, R. J Chem Phys 1992, 97, 2571.
52. Schäfer, A.; Huber, C.; Ahlrichs, R. J Chem Phys 1994, 100, 5829.
53. Slater, J. C. J Chem Phys 1964, 41, 3199.
54. Miertus, S.; Scrocco, E.; Tomasi, J. Chem Phys 1981, 55, 117.
55. Mennucci, B.; Cances, E.; Tomasi, J. J Phys Chem B 1997, 101, 10506.
56. Cammi, R.; Corni, S.; Mennucci, B.; Tomasi, J. J Chem Phys 2005, 122, 104513.
57. Rappe, A. K.; Casewit, C. J.; Colwell, K. S.; Goddard, W. A.; Skiff, W. M. J Am Chem Soc 1992, 114, 10024.
58. Cossi, M.; Barone, V. J Chem Phys 2001, 115, 4708.
59. Li, J.; Cramer, C. J.; Truhlar, D. G. Int J Quantum Chem 2000, 77, 264.
60. Ahlrichs, R.; Bär, M.; Häser, M.; Horn, H.; Kölmel, C. Chem Phys Lett 1989, 162, 165.
61. Gaussian 09, Revision A.1, Frisch, M. J.; Trucks, G. W.; Schlegel, H. B.; Scuseria, G. E.; Robb, M. A.; Cheeseman, J. R.; Scalmani, G.; Barone, V.; Mennucci, B.; Petersson, G. A.; Nakatsuji, H.; Caricato, M.; Li, X.; Hratchian, H. P.; Izmaylov, A. F.; Bloino, J.; Zheng, G.; Sonnenberg, J. L.; Hada, M.; Ehara, M.; Toyota, K.; Fukuda, R.; Hasegawa, J.; Ishida, M.; Nakajima, T.; Honda, Y.; Kitao, O.; Nakai, H.; Vreven, T.; Montgomery, Jr., J. A.; Peralta, J. E.; Ogliaro, F.; Bearpark, M.; Heyd, J. J.; Brothers, E.; Kudin, K. N.; Staroverov, V. N.; Kobayashi, R.; Normand, J.; Raghavachari, K.; Rendell, A.; Burant, J. C.; Iyengar, S. S.; Tomasi, J.; Cossi, M.; Rega, N.; Millam, N. J.; Klene, M.; Knox, J. E.; Cross, J. B.; Bakken, V.; Adamo, C.; Jaramillo, J.; Gomperts, R.; Stratmann, R. E.; Yazyev, O.; Austin, A. J.; Cammi, R.; Pomelli, C.; Ochterski, J. W.; Martin, R. L.; Morokuma, K.; Zakrzewski, V. G.; Voth, G. A.; Salvador, P.; Dannenberg, J. J.; Dapprich, S.; Daniels, A. D.; Farkas, Ö.; Foresman, J. B.; Ortiz, J. V.; Cioslowski, J.; Fox, D. J. Gaussian, Inc., Wallingford CT, 2009.
62. Serrano-Andres, L.; Merchan, M.; Borin, A. C. J Am Chem Soc 2008, 130, 2473.
63. Li, L.; Lubman, D. M. Anal Chem 1987, 59, 2538.
64. Clark, L. B.; Peschel, G. G.; Tinoco, I. J Phys Chem 1965, 69, 3615.
65. Du, H.; Fuh, R. C. A.; Li, J. Z.; Corkan, L. A.; Lindsey, J. S. Photochem Photobiol 1998, 68, 141.
66. Merchan, M.; Serrano-Andres, L. J Am Chem Soc 2003, 125, 8108.
67. Zaloudek, F.; Novros, J. S.; Clark, L. B. J Am Chem Soc 1985, 107, 7344.
68. Barbatti, M.; Aquino, A. J. A.; Lischka, H. PCCP 2010, 12, 4959.
69. Holmen, A.; Broo, A. Int J Quantum Chem 1995, 22, 113.
70. Fulscher, M. P.; Serrano-Andres, L.; Roos, B. O. J Am Chem Soc 1997, 119, 6168.
71. Serrano-Andres, L.; Merchan, M.; Borin, A. C. Chem—Eur J 2006, 12, 6559.
72. Fulscher, M. P.; Roos, B. O. J Am Chem Soc 1995, 117, 2089.
73. Blancafort, L.; Migani, A. J Photochem Photobiol Chem 2007, 190, 283.
74. Zhao, Y.; Truhlar, D. G. JCTC 2007, 3, 289.
75. Zhao, Y.; Truhlar, D. G. Acc Chem Res 2008, 41, 157.
76. Morgado, C. A.; Jurecka, P.; Svozil, D.; Hobza, P.; Sponer, J. PCCP 2010, 12, 3522.
77. Georgieva, I.; Trendafilova, N.; Aquino, A.; Lischka, H. J Phys Chem A 2005, 109, 11860.
78. Gao, J. L.; Xia, X. F. Science 1992, 258, 631.
79. Lin, H.; Truhlar, D. G. Theor Chem Acc 2007, 117, 185.
80. Senn, H. M.; Thiel, W. Angew Chem Int Ed Engl 2009, 48, 1198.